# Impact of a Semi-Lagrangian and an Eulerian Dynamical Core on Climate Simulations

MINGHANG CHEN,* RICHARD B. ROOD, AND LAWRENCE L. TAKACS†

*Data Assimilation Office, NASA/Goddard Space Flight Center, Greenbelt, Maryland*

(Manuscript received 1 November 1996, in final form 21 February 1997)

ABSTRACT

To assess the impact of dynamical formulation on climate simulations, a semi-Lagrangian and an Eulerian dynamical core have been used for 5-yr climate simulations with the same physical parameterizations. The comparison of the climate simulations is focused on various eddy statistics (the study of time-mean states from the simulations has been published in a previous paper). Significant differences between the two simulations are evident. Generally, the stationary eddy variances are stronger in the semi-Lagrangian simulation while the transient eddy variances are stronger in the Eulerian simulation. Compared to the data assimilated by the Goddard Earth Observing System data assimilation system, the semi-Lagrangian simulation is closer to the assimilation in many aspects than the Eulerian simulation, even though the Eulerian model was used in the data assimilation. The paper shows that rather than corrupting the ability to diagnose model performance with a parallel data assimilation, quantitative rigor can be advanced because the model environment is more controlled.

The two dynamical cores have been run for the idealized Held–Suarez tests to help understand the differences found in the climate simulations. The eddy statistics from the Held–Suarez tests are weaker and more diffused in the semi-Lagrangian than the Eulerian core. The transformed Eulerian mean diagnostics reveal that less wave activity propagates from the lower and middle troposphere into the upper troposphere in the semi-Lagrangian core. The residual circulation driven by eddy forcing is weaker in the semi-Lagrangian core than in the Eulerian core. Consequently, the semi-Lagrangian simulation is closer to the radiative equilibrium state than the Eulerian simulation. These diagnostics show that the different treatment of small-scale processes in the model (e.g., diffusion) profoundly impacts the simulation of the general circulation.

## 1. Introduction

Compared to the traditional Eulerian approach, the semi-Lagrangian approach has two principal advantages. The first is the ability to overcome the Courant–Friedrichs–Lewy (CFL) advective stability criterion. The second is the more accurate treatment of advection primarily by reducing phase dispersion errors for the finite-difference case (Bermejo 1990; Kuo and Williams 1990; Ostiguy and Laprise 1990). However, the semi-Lagrangian method also has two main disadvantages. The first is the absence of formal conservation properties. The second is that small-scale features may be damped more in semi-Lagrangian schemes than in some Eulerian schemes (McCalpin 1988). Staniforth and Côté (1991) have given a review of semi-Lagrangian schemes.

In view of increasing usage of the semi-Lagrangian method in general circulation models (GCMs) (e.g., Bates et al. 1993; Williamson and Olson 1994; Moorthi et al. 1995; Ritchie et al. 1995), it is important to investigate relative advantages and disadvantages of the semi-Lagrangian over the Eulerian approach in the context of both numerical weather prediction and climate simulation. Chen and Bates (1996b) have compared 10-day forecasts from a semi-Lagrangian and an Eulerian model with the same physical parameterizations. The result is that the two models produce the forecasts with similar skill scores even though the time step for the dynamics is 16 times longer in the semi-Lagrangian than in the Eulerian model. This has demonstrated the ability of a semi-Lagrangian model to achieve a significant improvement in efficiency of model integration without loss of accuracy [see Table 3 of Chen and Bates (1996b) for the CPU time comparison]. Also, Chen and Bates (1996a) have analyzed and compared 5-yr-mean climates simulated with the semi-Lagrangian and Eulerian models. It has been found that the change from an Eulerian to a semi-Lagrangian formulation leads to significant differences in the simulated climates, both for fields determined mainly by the dynamics, such as sea level pressure, and for those determined mainly by the physics, such as precipitation. The differences result both directly from the changes in the dynamics and

*Additional affiliation: Applied Research Corporation, Landover, Maryland.

† Additional affiliation: General Sciences Corporation, Laurel, Maryland.

*Corresponding author address:* Dr. Minghang Chen, Data Assimilation Office, NASA/Goddard Space Flight Center, 7501 Forbes Blvd., Suite 200, Seabrook, MD 20706.
E-mail: mchen@dao.gsfc.nasa.gov

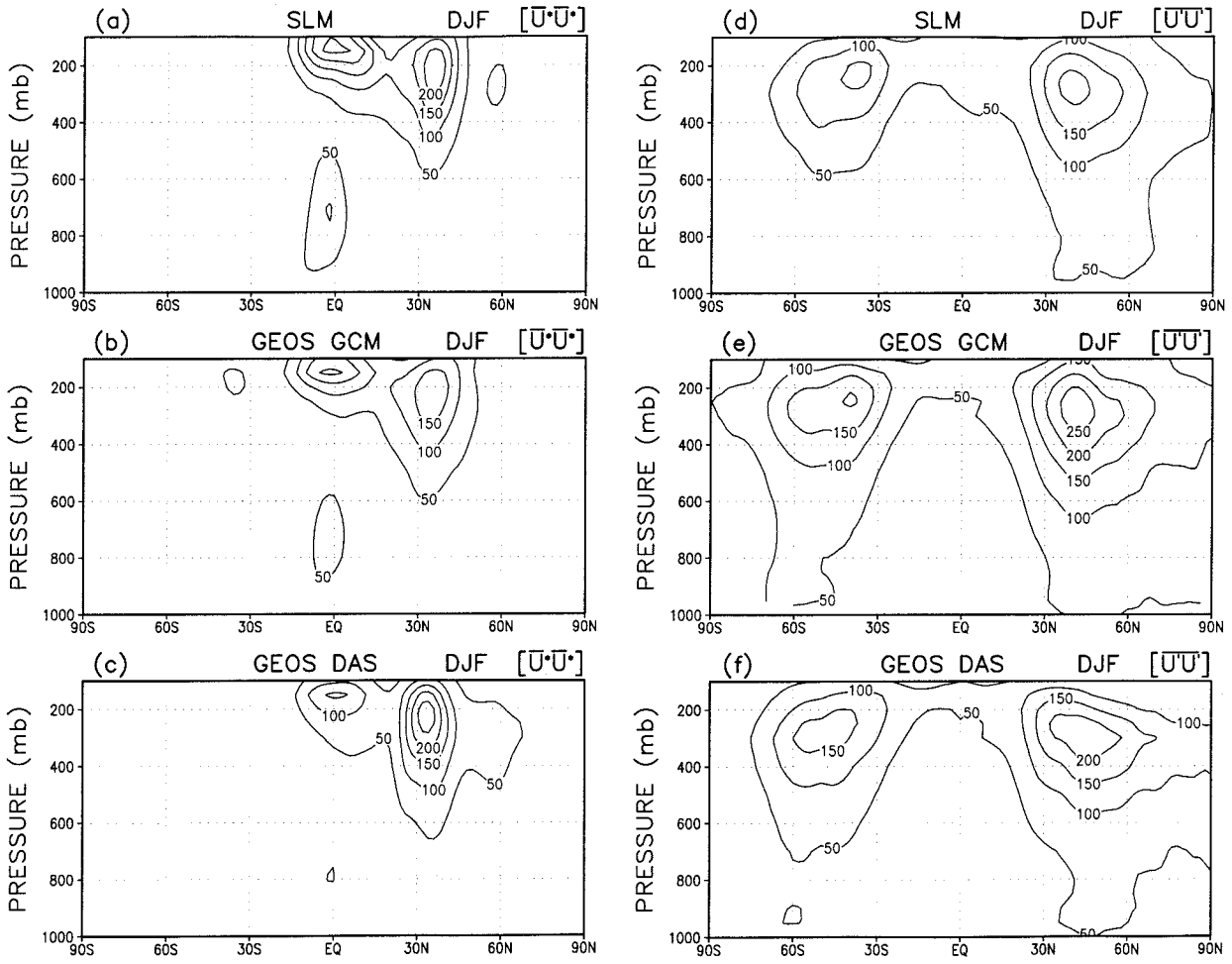


FIG. 1. Five-year-mean DJF stationary (a, b, and c), transient (d, e, and f), and total (g, h, and i) eddy variance of zonal wind from the simulations and assimilation. The contour interval is 50 $m^2 s^{-2}$.

indirectly from the interactions of the dynamics with the physics, even though the same physical parameterizations are used in the two models.

The comparison of the climate simulations in Chen and Bates (1996a) is focused on the time-mean states. In this study, the eddy statistics from the same climate simulations are compared. In addition, the two models have been run for the benchmark test proposed by Held and Suarez (1994). This test uses simple Newtonian relaxation for the temperature field and Rayleigh damping for low-level winds without any explicit physical parameterizations. Running the test is an attempt to isolate differences solely due to the different formulations of the dynamics. Then the transformed Eulerian mean diagnostics are employed for the Held–Suarez test to track down differences between the dynamical cores. Concomitantly, the comparison of the long-term statistics from the test with those from the climate simulations would provide some implication on the usefulness of the Held–Suarez test for dynamical core comparison. In total, the experiments undertaken here are focused on trying to better quantify the factors in the models that lead to different performance. This is a necessary step in the quest to better define uncertainties in climate simulation and prediction.

Brief descriptions of the models are given in section 2. Eddy statistics from the climate simulations are presented in section 3. Results from the Held–Suarez tests are given in section 4. Section 5 gives the comparison of the climate and idealized simulations and the interpretation of results using the transformed Eulerian mean framework. Finally, the conclusions are given in section 6.

## 2. Brief model descriptions

The dynamical core of the semi-Lagrangian model (SLM) is described in Bates et al. (1993). It uses a two-time-level semi-implicit finite-difference integration scheme. The integration scheme is an extension of the vector semi-Lagrangian scheme of Bates et al. (1990)

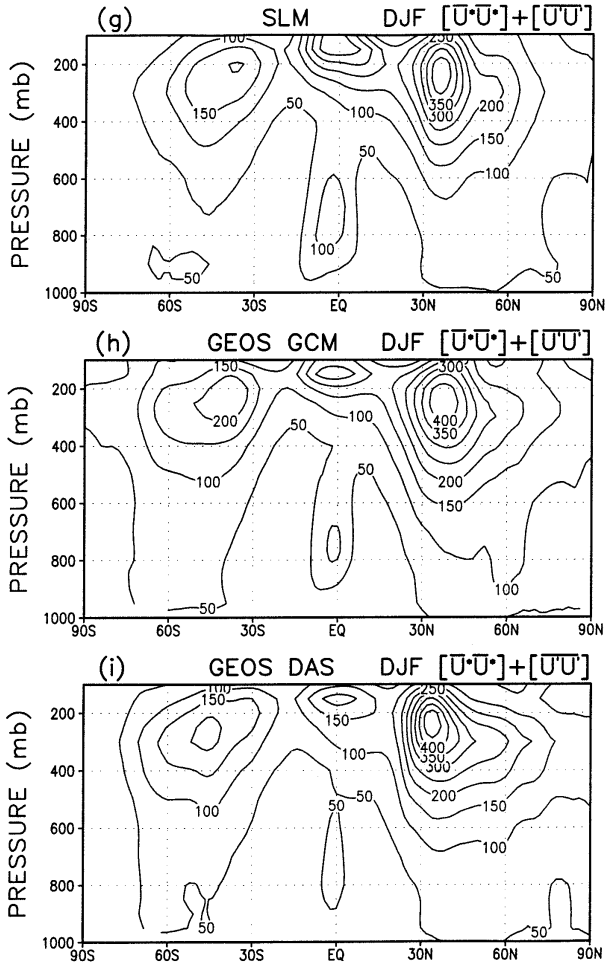


FIG. 1. (*Continued*)

to the multilevel case. Values of variables at trajectory departure points are evaluated using tricubic interpolation, which gives fourth-order spatial accuracy for horizontal and vertical advection. The order of accuracy of the vertical advection is not reduced by the unequal spacing of levels. A few modifications to the original dynamical core of Bates et al. (1993) are described by Moorthi et al. (1995) and Chen and Bates (1996a).

The Eulerian model is the Goddard Earth Observing System (GEOS) GCM (Takacs et al. 1994), which has been used in the data assimilation system (DAS) at the Data Assimilation Office (DAO), NASA/Goddard Space Flight Center (Schubert et al. 1993). The Eulerian dynamical core is described by Suarez and Takacs (1995). The version used in the climate simulation is the first version of the dynamical core, which has second-order accuracy in horizontal differencing, but the latest version with fourth-order accuracy is used for the Held–Suarez test. Section 4 gives the justification for linking the comparison of the climate simulations with the comparison of the Held–Suarez tests despite the two different versions used. The vertical differencing follows the scheme developed by Arakawa and Suarez (1983), which is second-order accurate where the levels are equally spaced, but reduces to first-order accuracy where unequal spacing occurs. In one-dimensional advection by a constant velocity the semi-Lagrangian and Eulerian dynamical cores perform similarly to each other.

Version 1 of the GEOS GCM physical parameterizations (Takacs et al. 1994) is used in both models. The turbulence parameterization consists of components that handle vertical diffusion and surface fluxes of heat, moisture, and momentum (Helfand and Labraga 1988). The relaxed Arakawa–Schubert (RAS) scheme (Moorthi and Suarez 1992) is used to parameterize moist convection. A parameterization of rain reevaporation (Sud and Molod 1988) is also included. The longwave and shortwave radiation schemes closely follow those of Harshvardhan et al. (1987). Convective and large-scale (layered) clouds are diagnosed in the parameterizations of moist convection and large-scale condensation. A time split method is used in the semi-Lagrangian model to incorporate the Eulerian physics (see Chen and Bates 1996a).

The semi-Lagrangian and Eulerian models were integrated for 5 yr (1985–90) at horizontal resolution of $2^\circ$ lat $\times$ $2.5^\circ$ long with 20 vertical levels unequally spaced. The time step for the dynamics is 60 min for the SLM and 2.5 min for the GEOS GCM. The uncentering parameter $\epsilon = 0.2$ is used in the SLM. The time step and the value of $\epsilon$ in the SLM are chosen based on a series of forecast experiments. These values of the time step and $\epsilon$ give the best overall forecast scores (Chen and Bates 1996b). The CPU time comparison for the two models are given in Table 2 of Chen and Bates (1996a). More detailed descriptions of the integrations have been given by Chen and Bates (1996a) and Takacs and Suarez (1996). The validation dataset is the assimilation for the same time period from the GEOS DAS (Schubert et al. 1993, 1995). While the use of the GEOS DAS, which used the GEOS GCM, might seem to favor the GEOS GCM simulation, such an advantage is not obviously realized (see section 3).

## 3. Eddy statistics from climate simulations

The eddy statistics from the simulations and assimilation are initially calculated on the basis of monthly means. These statistics from monthly means are averaged to generate the 5-yr-mean seasonal eddy statistics for the December–February (DJF) and June–August (JJA) seasons. Thus, the stationary eddy variances are the variances due to the eddies with timescales equal to or longer than one month. For fields $x$ and $y$ the eddy statistics are defined by

$$[\overline{xy}] = [\bar{x}][\bar{y}] + [\bar{x}^*\bar{y}^*] + [\overline{x'y'}], \qquad (1)$$

where the bar denotes the monthly mean, the prime the

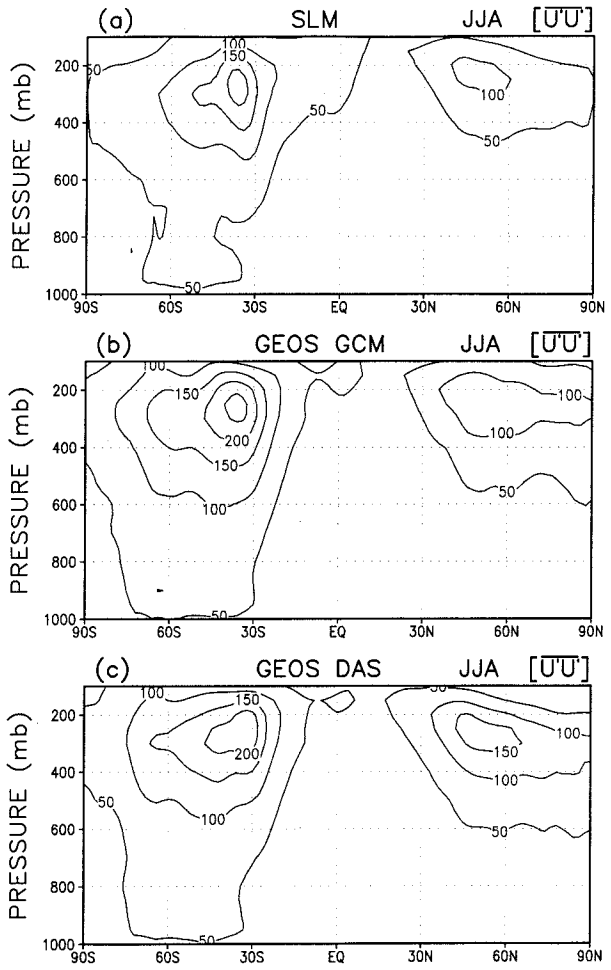


FIG. 2. Five-year-mean JJA transient eddy variance of zonal wind from the simulations and assimilation. The contour interval is 50 $m^2$ $s^{-2}$.

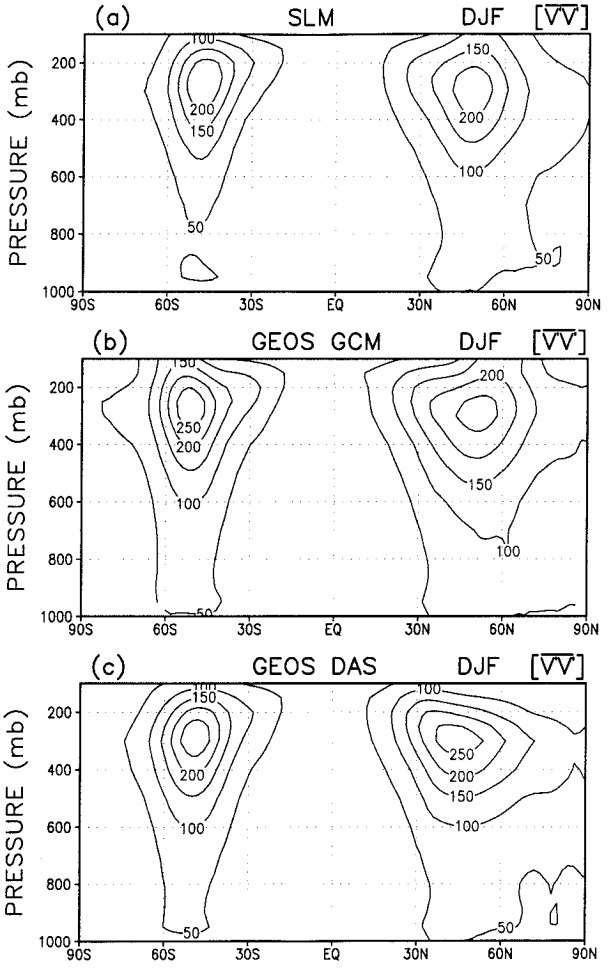


FIG. 3. Five-year-mean DJF transient eddy variance of meridional wind from the simulations and assimilation. The contour interval is 50 $m^2$ $s^{-2}$.

deviation from the monthly mean, the bracket the zonal mean, and the asterisk the deviation from the zonal mean. The second and third terms on the right-hand side are the stationary and transient eddy variance, respectively. The total eddy variance is simply the sum of the two.

Figure 1 shows the DJF stationary, transient, and total eddy variances of zonal wind. The stationary eddy variance (Figs. 1a–c) in the Northern Hemisphere (NH) midlatitudes is stronger in the SLM than in the GEOS GCM. Both simulations are weaker than the assimilation; therefore, the SLM simulation is closer to the GEOS DAS. The simulated stationary variances in the Tropics are stronger than the GEOS DAS, especially in the SLM. The NH transient eddy variance (Figs. 1d–f) simulated by the SLM is also closer to the assimilation than that simulated by the GEOS GCM. In the Southern Hemisphere (SH) midlatitudes, the GEOS GCM simulation is stronger than the SLM simulation and closer to the GEOS DAS. Due to the opposite differences in the stationary and transient variances, the total eddy variance (Figs. 1g–i) in the NH midlatitudes is similar in the two simulations, both of which are weaker than the assimilation. For JJA, only the transient eddy variances are shown (Fig. 2). In the NH midlatitudes, the two simulations are weaker than the assimilation. The maximum variance in the SH midlatitudes is too strong in the GEOS GCM, and it is more consistent with the assimilation in the SLM. The JJA stationary eddy variance (not shown) is small in the extratropics of both hemispheres.

The DJF transient eddy variance of meridional wind is shown in Fig. 3. The GEOS GCM simulation is stronger than the SLM simulation and in better agreement with the assimilation. Figure 4 shows the JJA transient eddy variance of meridional wind. For both hemispheres the GEOS GCM simulation is again stronger than the SLM simulation, which makes the GEOS GCM simu-

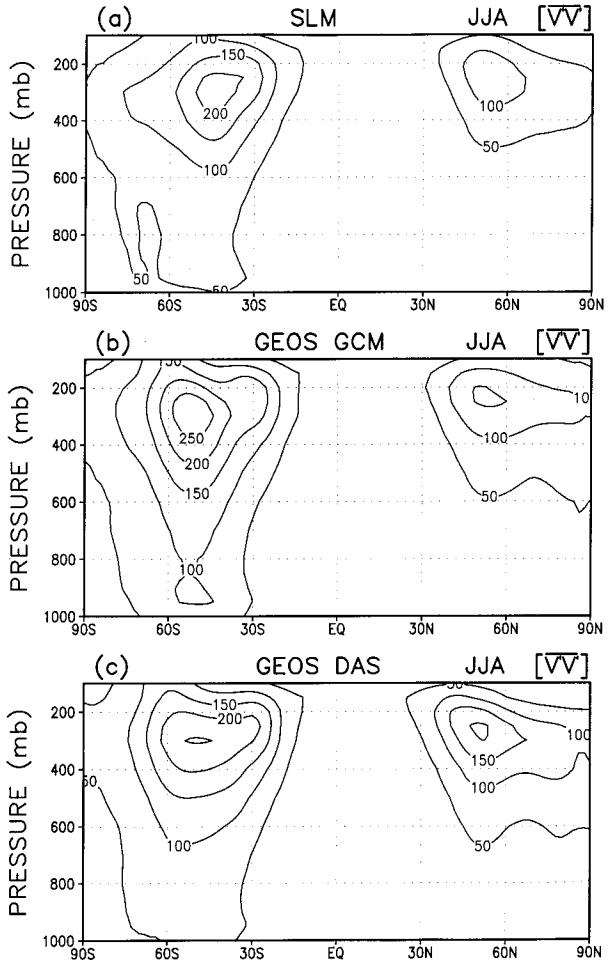


FIG. 4. Same as Fig. 3 but for JJA.

lation closer to the assimilation. The stationary eddy variances of meridional wind are small (not shown) for both seasons.

Figure 5 shows the DJF stationary, transient, and total eddy flux of momentum. The positive center in the stationary eddy flux (Figs. 5a–c) in the NH midlatitudes is better simulated by the SLM than by the GEOS GCM, which overestimates the flux. In the tropical upper troposphere the SLM simulation is too strong. Neither simulation captures the negative center visible in the GEOS DAS north of 60°N. The transient eddy flux (Figs. 5d–f) in the SH is very similar in the two simulations, and both models overestimate the transient flux by more than 30%. In the NH, the transient eddy flux is overestimated by about 50% in the GEOS GCM and by about 35% in the SLM. The NH maximum of the transient flux is located too northward in the simulations. The total eddy momentum flux (Figs. 5g–i) in the NH midlatitudes is significantly stronger in the GEOS GCM than in the SLM, with the SLM simulation closer to the assimilation. At the latitudes around 65° of both hemispheres the total eddy flux is underestimated by the models. Figure 6 shows the JJA transient eddy momentum flux. The two simulations in the NH midlatitudes are closer to each other than to the assimilation; both are stronger than the assimilation. For the SH, the transient flux is better simulated by the SLM. The JJA stationary momentum flux (not shown) is very small in the extratropics. In the Tropics, it is overestimated by the SLM.

The DJF eddy heat flux is presented in Fig. 7. The stationary eddy flux (Figs. 7a–c) is significant only in the NH midlatitudes. The two simulations are more similar to each other than to the assimilation; both are weaker than the assimilation. The transient eddy heat flux is shown in Figs. 7d–f. Compared with the assimilation, the transient eddy flux is generally overestimated by the models. For the lower troposphere in the NH extratropics the simulation is stronger in the GEOS GCM than in the SLM, while the two simulations in the SH are close to each other. Figures 7g–i show the total eddy heat flux. The simulations are basically consistent with the assimilation, demonstrating a compensation of errors in the transient and stationary components. It is interesting that the GEOS GCM simulation has a maximum near the midlatitude tropopause of each hemisphere, which is not as well defined in the SLM simulation. The NH maximum is found in the assimilation while the SH one is not. Figure 8 shows the JJA transient eddy heat flux. Large values of the heat flux are found only in the SH extratropics. The SLM simulation is weaker than the GEOS GCM simulation, and the SLM is in better agreement with the assimilation. Again, the JJA stationary eddy heat flux is very small and not shown.

## 4. Held–Suarez test

Held and Suarez (1994) have proposed an idealized test to investigate dynamical formulations used in GCMs. We use this test to try and understand the differences in the climate simulations. The test uses thermodynamic and momentum equations with specified forcing to yield a circulation that is grossly similar to the observed tropospheric circulation. The thermal forcing is linear relaxation to a specified temperature field varying with latitude and pressure, which assures that the wind fields have jets in the subtropical upper troposphere. There is a momentum sink represented by Rayleigh friction at the lower troposphere. The friction and thermal forcing assure a mean meridional circulation that is broadly consistent with a Hadley cell rising in the Tropics and descending outside of the Tropics. There is no attempt made to resolve or model the stratosphere. No topography is included in the test, and symmetry is expected between the NH and the SH. A major difference between the atmospheric circulation and the Held–Suarez circulation is that the Hadley circulation in the atmosphere is maintained by direct heating while it is not the case in the Held–Suarez test. This will be exploited in the interpretation in the next section.

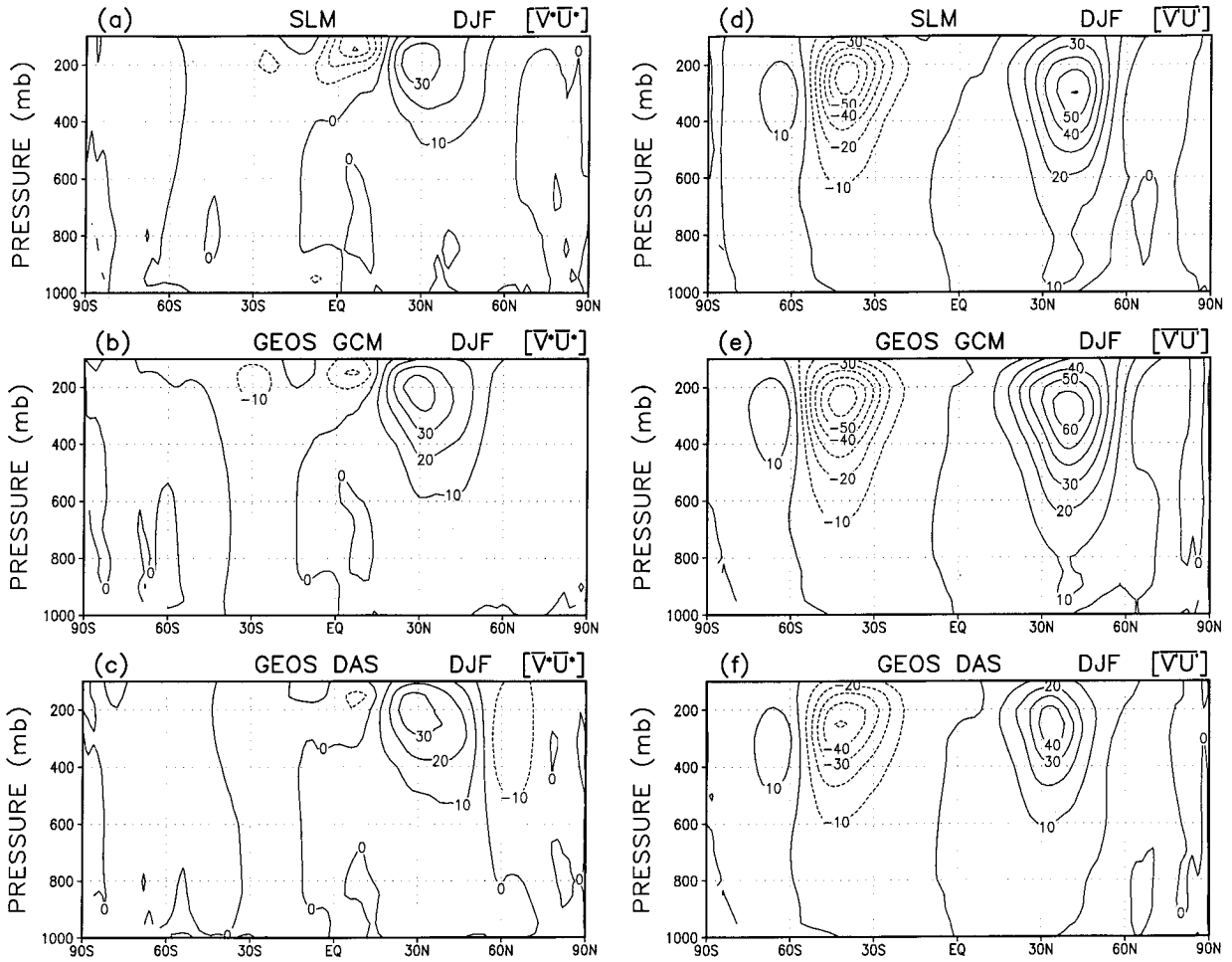


FIG. 5. Five-year-mean DJF stationary (a, b, and c), transient (d, e, and f), and total (g, h, and i) eddy momentum flux from the simulations and assimilation. The contour interval is 10 $m^2$ $s^{-2}$.

Both SLM and GEOS dynamical cores were run at horizontal resolution of 2° lat × 2.5° long with 20 $\sigma$ levels equally spaced, where $\sigma = p/p_s$, $p$ is the pressure, and $p_s$ is the surface pressure. The time step is 60 min for the SLM and 3.75 min for the GEOS. For these time steps the CPU time for the SLM core is about one-half of that for the GEOS core. The reduction in CPU time is far less than that expected from the increase in the time step. This is due partly to the semi-Lagrangian overhead, and partly to the fact that the SLM has not been optimized for CPU-time performance. As in the climate simulation, the uncentering parameter $\epsilon = 0.2$ is used in the SLM. The initial state used for the model integrations is derived from a European Centre for Medium-Range Weather Forecasts (ECMWF) analysis, and thus it is asymmetric about the equator. The models were integrated for 1200 days. The time-mean fields and eddy statistics are taken from the last 1000 days. Since there is no topography and surface contrast, the stationary eddy components are small and the total eddy statistics are similar to the transient eddy components.

The Eulerian core used for the Held–Suarez test is the latest version, which has fourth-order accuracy in horizontal advection, while the version used for the climate simulation is second-order accurate in horizontal advection. Comparison of the present results with those described by Held and Suarez (1994), who used the same Eulerian core with second-order accuracy, clearly shows that the differences between the Held–Suarez integrations with the second-order and fourth-order Eulerian cores are small compared to the differences between the semi-Lagrangian and Eulerian cores. Additional experiments have also confirmed this. Furthermore, the differences in the climate simulations using the second-order and fourth-order Eulerian core at the resolution of 2° lat × 2.5° long (Takacs and Suarez 1996) are small compared to the corresponding differences between the semi-Lagrangian

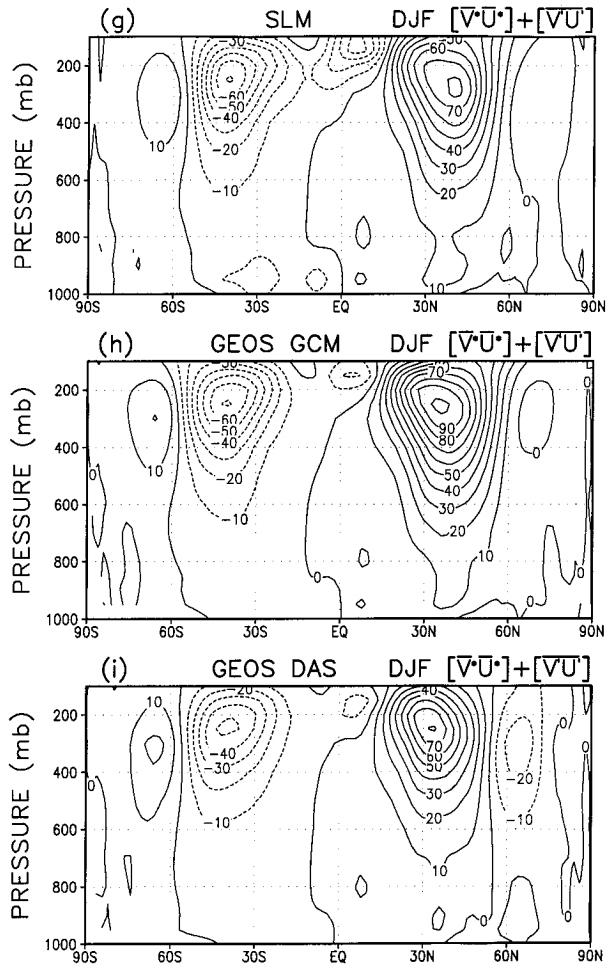


FIG. 5. (*Continued*)

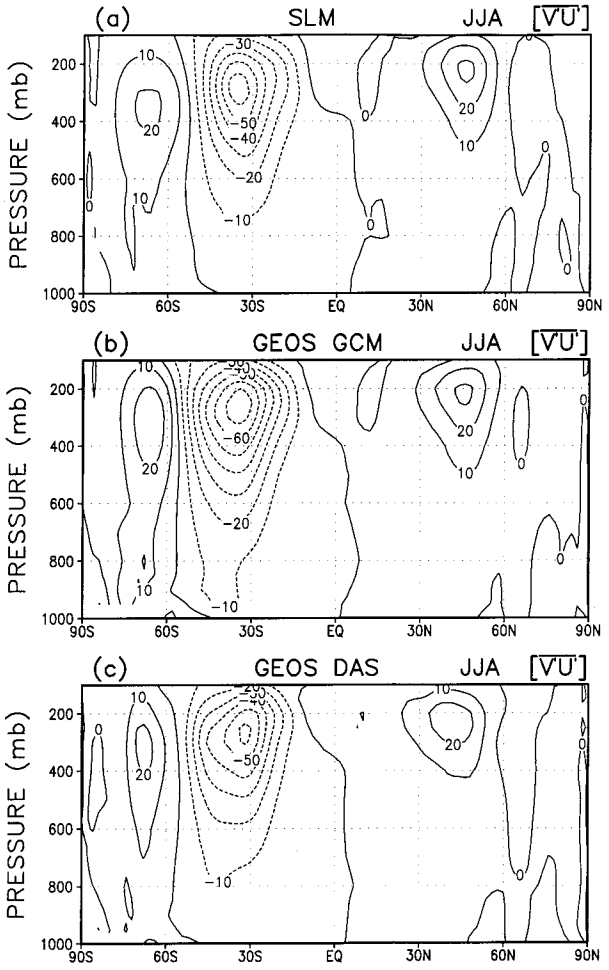


FIG. 6. Five-year-mean JJA transient eddy momentum flux from the simulations and assimilation. The contour interval is 10 $m^2$ $s^{-2}$.

and Eulerian models (Chen and Bates 1996a). Thus, it is justified to link the comparison of the climate simulations with the comparison of the Held and Suarez tests, even though the two different versions of the Eulerian core were used.

The zonal-mean time-mean zonal wind from the SLM and GEOS cores is shown in Fig. 9. The maximum westerlies in midlatitudes are slightly stronger in the SLM than in the GEOS. The upper-level easterlies in the Tropics are considerably stronger in the GEOS than in the SLM. In the climate simulation with the GEOS GCM the strong tropical easterlies are found in the summer season but not in the winter (Chen and Bates 1996a). Figure 10 shows the zonal-mean meridional wind produced by the two cores. The two simulations are generally similar. The meridional wind implies the vertical motion of a Hadley cell, with strong ascent in the Tropics and descent in the subtropics. The maximum meridional winds in the lower and upper tropical troposphere are slightly stronger in the GEOS than in the SLM, which implies stronger tropical vertical motion in the GEOS. It is further discussed in section 5 in the context of the residual circulation.

Figure 11 shows the simulated temperature fields and their differences. The significant differences are found at the levels above $\sigma = 0.25$ (Fig. 11c). The tropical tropopause is warmer by 6 K in the SLM than in the GEOS. At high latitudes of both hemispheres, however, the SLM simulation is 6–8 K colder than the GEOS simulation at those levels above $\sigma = 0.25$ and about 2 K colder at the levels below. This is opposite to the result found in the climate simulations by Chen and Bates (1996a). The climate simulations show that the temperature in the upper troposphere and the lower stratosphere in high latitudes is significantly warmer in the SLM while the temperature in the Tropics is similar in the two models. The different results are due to the fact that the processes that maintain circulation and temperature structure in the Held–Suarez test are very different from those in the real climate simulations. The

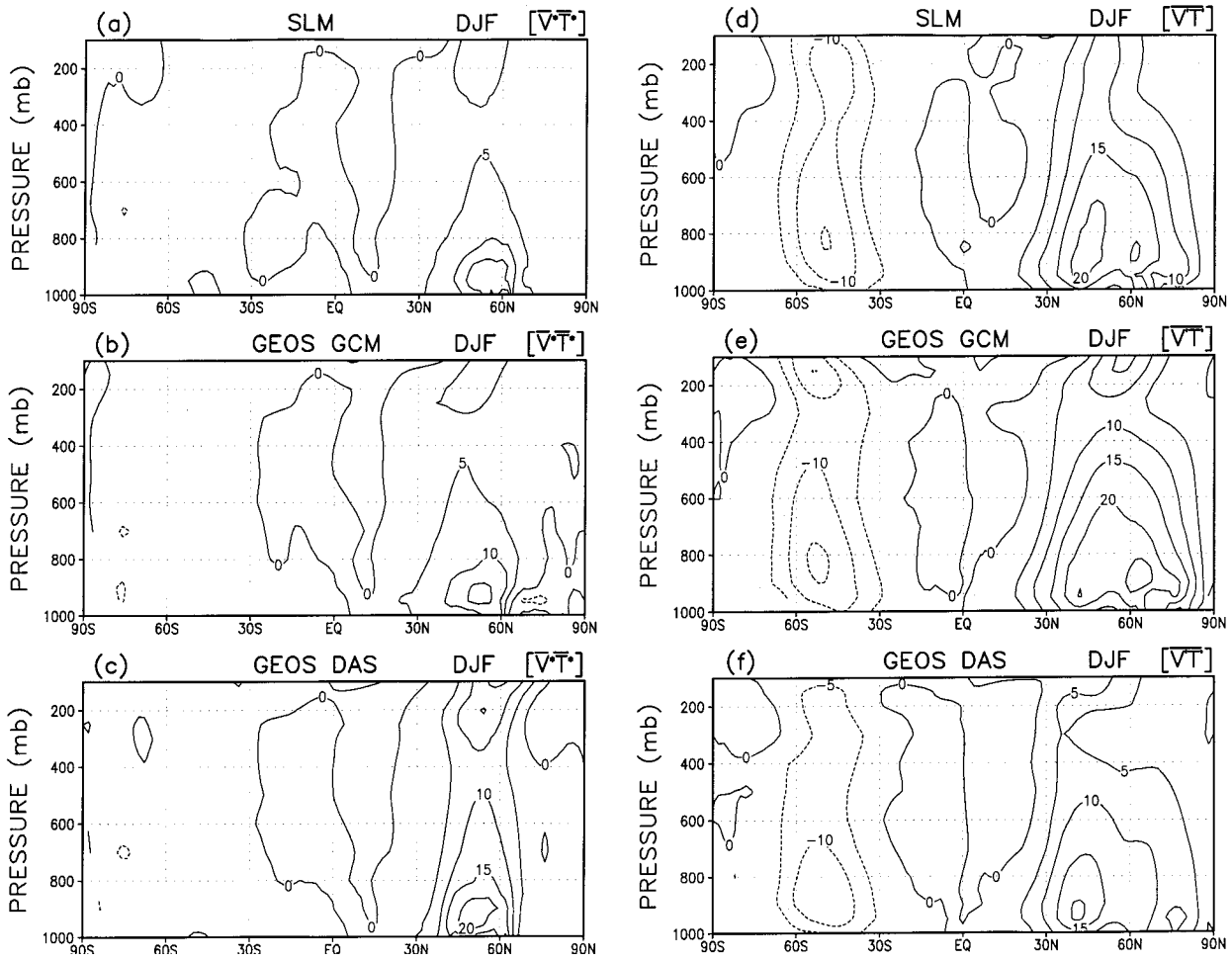


FIG. 7. Five-year-mean DJF stationary (a, b, and c), transient (d, e, and f), and total (g, h, and i) eddy heat flux from the simulations and assimilation. The contour interval is 5 K m $s^{-1}$.

long-term states of simulations critically depend on employed processes (see Boer and Denis 1997 for some experiments). This will be further discussed in section 5.

The eddy variance of the zonal wind is shown in Fig. 12. The two models generate similar latitudinal and vertical distributions of the variance. Two maxima are found in midlatitudes at the level of $\sigma = 0.275$. However, the eddy variance in the SLM is only about a half of that in the GEOS. The eddy variances of meridional wind and temperature are also substantially weaker in the SLM than in the GEOS (not shown). The weaker eddy variances in the SLM may be associated with the much longer time step (1 h vs 3.75 min), the uncentering parameter $\epsilon = 0.2$, and possible damping effect due to the interpolation in the SLM core. We have also run the SLM core for the Held–Suarez test with $\epsilon = 0$. The eddy variances with $\epsilon = 0$ are stronger than those with $\epsilon = 0.2$. But even with $\epsilon = 0$, the SLM eddy variances are much weaker than those from the GEOS core.

Figure 13 shows the eddy momentum flux. The only difference between the two integrations is that the SH maximum is stronger in the SLM than in the GEOS, with the indication of higher hemispheric symmetry in the SLM. The asymmetry reflects sampling errors since the forcing is symmetric. Figure 14 shows the eddy heat flux. The two models give very similar latitudinal and vertical distributions of the field. There are two maxima in midlatitudes of each hemisphere, one in the lower troposphere and another in the upper troposphere. The maxima of eddy heat flux are weaker in the SLM than in the GEOS.

## 5. Comparison and synthesis

Comparison of the Held–Suarez test results with the climate simulations using the two different dynamical cores provides direction for understanding the impact of the dynamical cores on the model results. To carry the comparison beyond a description of averaged diagnostics, the results will be interpreted using the trans-

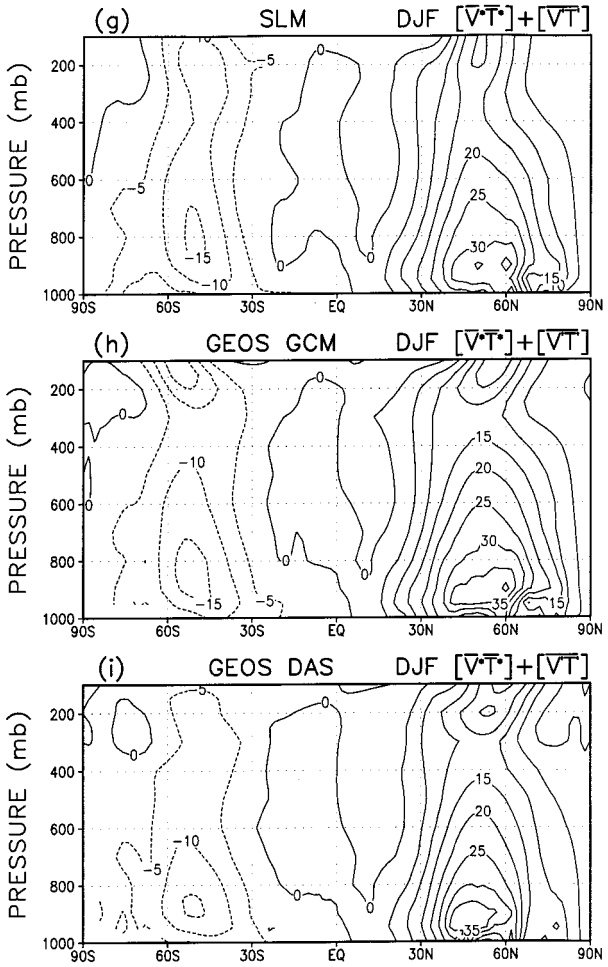


FIG. 7. (*Continued*)

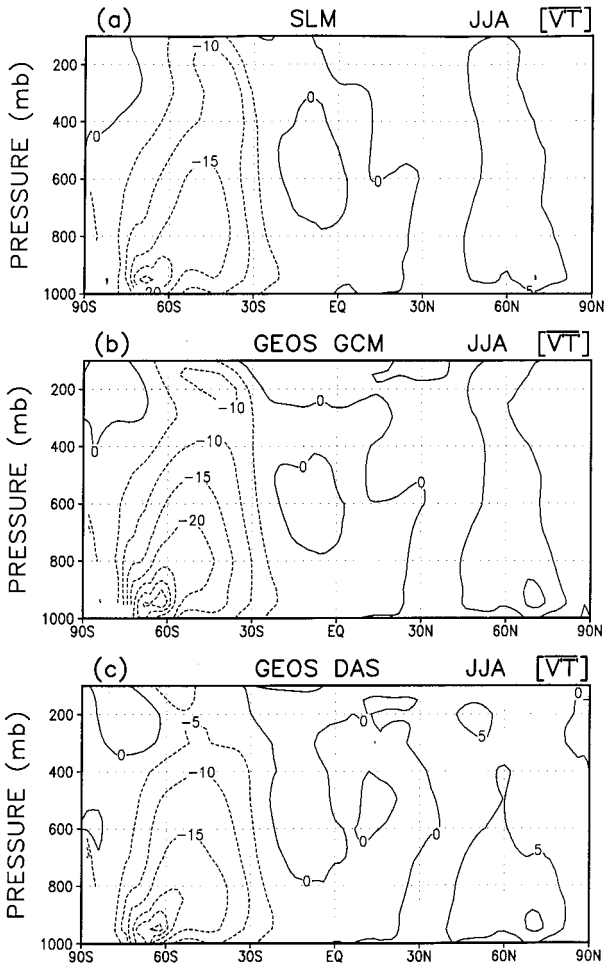


FIG. 8. Five-year-mean JJA transient eddy heat flux from the simulations and assimilation. The contour interval is 5 K m $s^{-1}$.

formed Eulerian mean (TEM) framework as used, for instance, in Edmon et al. (1980) and Plumb and Mahlman (1987) (see World Meteorological Society 1986 for an excellent summary).

As argued by Fels et al. (1980) and others, in order for the atmosphere to equilibrate at temperatures different from radiative equilibrium, a balance between eddy wave motions and a wave-driven mean meridional circulation (the transformed Eulerian mean or, commonly, the residual circulation) must exist. The vertical component of the mean circulation drives the atmosphere away from radiative equilibrium by cross-isentropic transport. This is balanced by quasi-horizontal mixing along isentropes, which brings the atmosphere towards radiative equilibrium. In the stratospheric applications, where the TEM framework has been used the most, the tropical upward and polar downward components of the mean meridional circulation are forced at a distance by the dissipation of Rossby and gravity waves that have propagated into the upper stratosphere and mesosphere (see Haynes et al. 1991; Holton et al. 1995 and references therein). The processes that maintain the mean meridional circulation in the Held–Suarez test are due to similar action-at-a-distance mechanisms, rather than direct heating as in the atmospheric Hadley circulation. Therefore, the use of the TEM framework is expected to be productive. The focus will be on the propagation of waves from the lower part of the model to the upper part of the model, where they are dissipated by Newtonian cooling.

The primary underlying assumption of the TEM formulation is quasigeostrophy. With the residual circulation ($v_*$, $w_*$) defined by (see Andrews and McIntyre 1976; Andrews et al. 1987; Holton 1992)

$$\bar{v}_* = \bar{v} - \frac{R}{\rho_o H}\frac{\partial}{\partial z}\left(\frac{\rho_o}{N^2}\overline{v'T'}\right) \tag{2}$$

$$\bar{w}_* = \bar{w} + \frac{R}{Ha\cos\phi}\frac{\partial}{\partial\phi}\left(\frac{\cos\phi}{N^2}\overline{v'T'}\right), \tag{3}$$

the TEM equations can be written as

$$\frac{\partial \bar{u}}{\partial t} - f\bar{v}_* = \frac{1}{\rho_o a \cos\phi}\nabla\cdot\mathbf{F} + \bar{X} \tag{4}$$

$$\frac{\partial \bar{T}}{\partial t} + \frac{HN^2}{R}\bar{w}_* = \bar{Q} \tag{5}$$

$$\frac{1}{a\cos\phi}\frac{\partial}{\partial\phi}(\bar{v}_*\cos\phi) + \frac{1}{\rho_o}\frac{\partial}{\partial z}(\rho_o\bar{w}_*) = 0 \tag{6}$$

$$\mathbf{F} = (F_\phi, F_z) = \left(-\rho_o a\cos\phi\overline{v'u'},\ \rho_o a\cos\phi\frac{Rf}{HN^2}\overline{v'T'}\right), \tag{7}$$

where

$$N^2 = \frac{R}{H}\left(\frac{\kappa\bar{T}}{H} + \frac{\partial\bar{T}}{\partial z}\right)$$

$$z = -H\ln\frac{p}{p_o}$$

$$\rho_o = \frac{p_o}{gH}e^{-z/H}$$

$$\kappa = \frac{R}{c_p}.$$

In the above, $a$ is the earth radius, $g$ the gravity acceleration, $R$ the gas constant for dry air, $c_p$ the specific heat of dry air at constant pressure, $\phi$ the latitude, $f$ the Coriolis parameter, $u$ the zonal wind, $v$ the meridional wind, $w$ the vertical velocity, $T$ the temperature, $X$ the subgrid-scale momentum forcing, $Q$ the diabatic heating, the scale height $H = 7$ km, the reference pressure $p_o = 1000$ mb, and $\mathbf{F}$ the vector Eliassen–Palm (EP) flux. The bar denotes the zonal mean and the prime the deviation from the zonal mean.

Since the Held–Suarez test does not have a substantive stationary wave component, the transient component in the climate simulations will be examined. Here we focus on the comparison of the Held–Suarez test with the DJF climate simulation in the NH. Comparison of the variance of the zonal wind (Figs. 1d and 1e with Fig. 12) shows the Held–Suarez simulations have features in common with the climate simulations. The magnitude of the variance in the Held–Suarez test is greater (less) than the climate simulation for the GEOS (SLM) core. Thus, the differences found in the Held–Suarez tests between the two cores are larger than those found in the climate simulations. The latitudinal extent of the contours at the height of the maximum in both the climate and the idealized simulations is more compact than in the assimilation field shown in Fig. 1f. The poleward extent of the 50 $m^2\ s^{-2}$ contour in the GEOS simulation of the Held–Suarez test (Fig. 12b), and the similar structure in the GEOS climate simulation (Fig. 1e), show a tendency for more polar variance in the GEOS core.

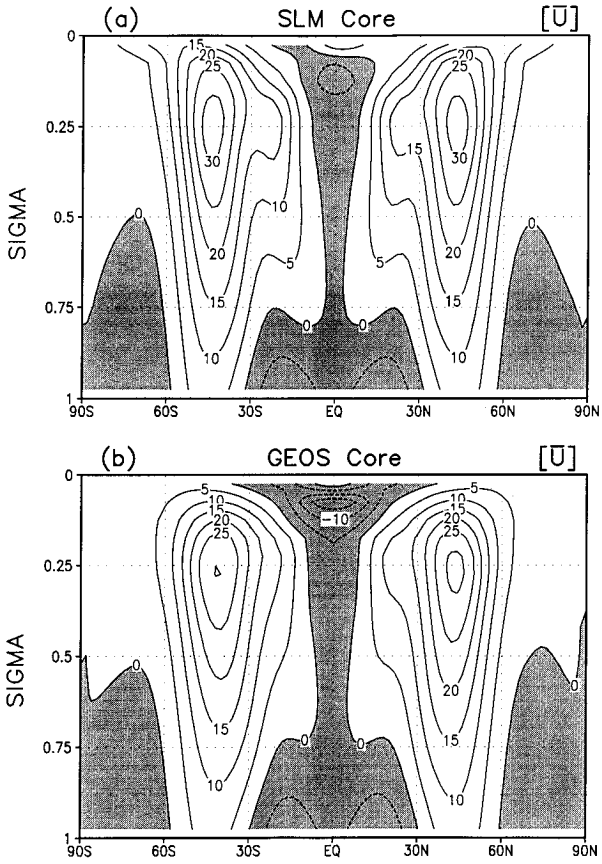


FIG. 9. Time-mean zonal wind from the Held-Suarez tests with the (a) SLM and (b) GEOS dynamical cores. The contour interval is 5 m $s^{-1}$ with negative values shaded.

Compared with the GEOS model the variance in the SLM looks more diffused.

The meridional momentum fluxes (Figs. 5d and 5e with Fig. 13) are similar. The heat fluxes (Figs. 7d and 7e with Fig. 14) are more revealing. Both representations of the Held–Suarez test show two peaks, one in the lower troposphere and one in the upper troposphere. This is similar to the GEOS GCM climate simulation. The assimilation (Fig. 7f) and the SLM climate simulation (Fig. 7d) do not show as distinct a double maximum. In the Held–Suarez tests the peaks in the GEOS core are both of greater magnitude and more distinctly separated. Once again, the SLM solution looks more diffused. Since the heat flux is proportional to the vertical component of the EP flux [see (7)], there is a difference in the propagation of waves from the lower to the upper parts of the model. Figure 15 shows the EP flux from the Held–Suarez tests. Indeed, the vertical component of the EP flux is weaker in the SLM (Fig. 15c). Thus, in the SLM less wave activity is propagating into the upper troposphere from the primary source region in the middle and lower troposphere at midlati-

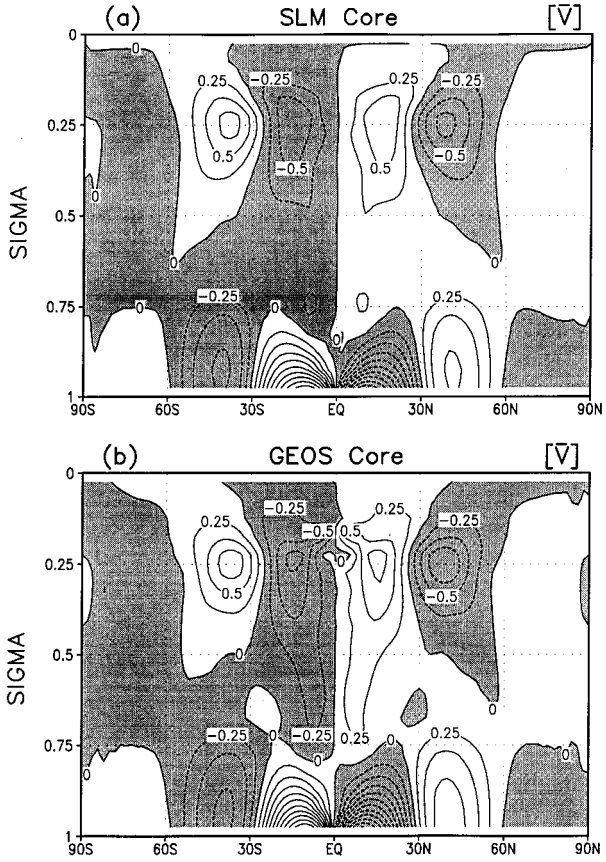


FIG. 10. Time-mean meridional wind from the Held-Suarez tests with the (a) SLM and (b) GEOS dynamical cores. The contour interval is 0.25 m $s^{-1}$ with negative values shaded.

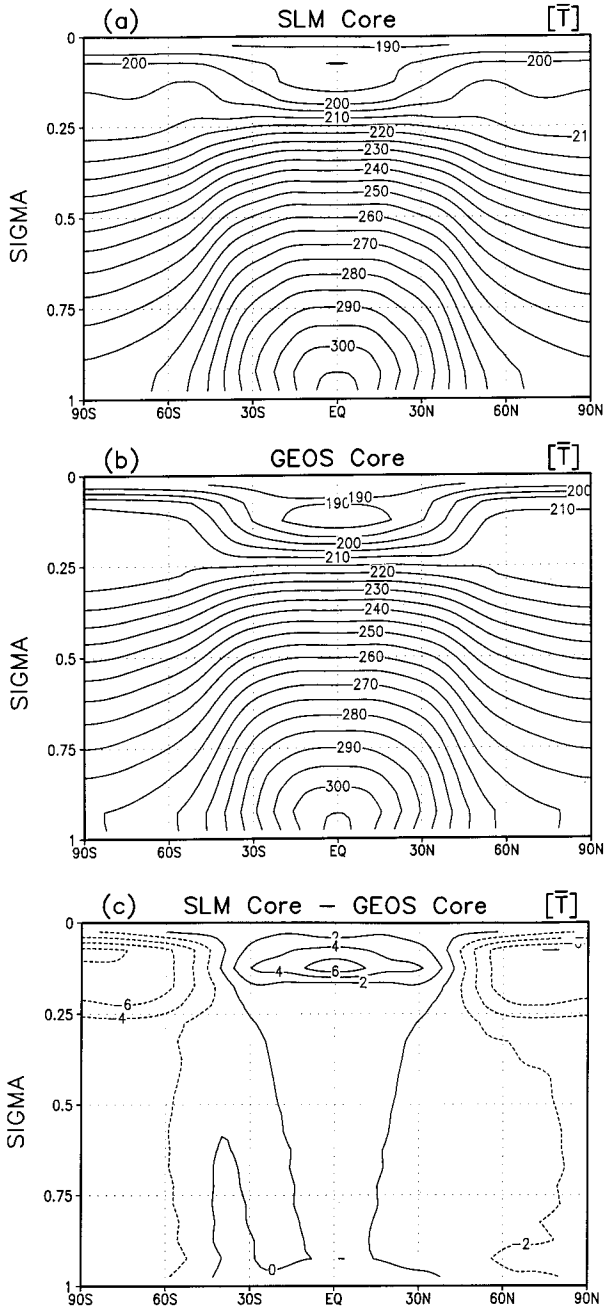


FIG. 11. Time-mean temperature from the Held-Suarez tests with the (a) SLM and (b) GEOS dynamical cores, and (c) their difference (SLM − GEOS). The contour interval is 5 K in (a) and (b) and 2 K in (c).

tudes. Also, less wave activity propagates equatorward in the upper troposphere.

A weaker residual circulation is expected since less wave activity is dissipated at high altitudes in the SLM core. Figure 16 shows the meridional and vertical components of the residual circulation from the two simulations. The vertical component of the residual circulation (Figs. 16c and 16d) is indeed weaker in the SLM core than in the GEOS core. The most obvious differences are at the equator and the poles as well as at 30° in the upper troposphere. The vertical component of the residual circulation does suggest a direct Hadley cell in the Tropics as well as a mean meridional circulation around the subtropical jet. The largest differences in the meridional component of the residual circulation (Figs. 16a and 16b) are in the upper troposphere between the equator and 30°.

The stronger residual circulation implies that the GEOS core will be farther away from radiative equilibrium and, hence, warmer at the poles than the SLM core. Figure 17 shows the difference between the average modeled temperature and the radiative equilibrium temperature from the Held–Suarez tests. At the poles, the SLM dynamical core is colder than the GEOS core and closer to radiative equilibrium by approximately 3 K just above $\sigma = 0.5$. At higher altitudes where the temperature differences between the two cores are largest (Fig. 11c), the SLM core is more than 6 K closer to radiative equilibrium than the GEOS core. At the equator, the SLM is also closer to radiative equilibrium

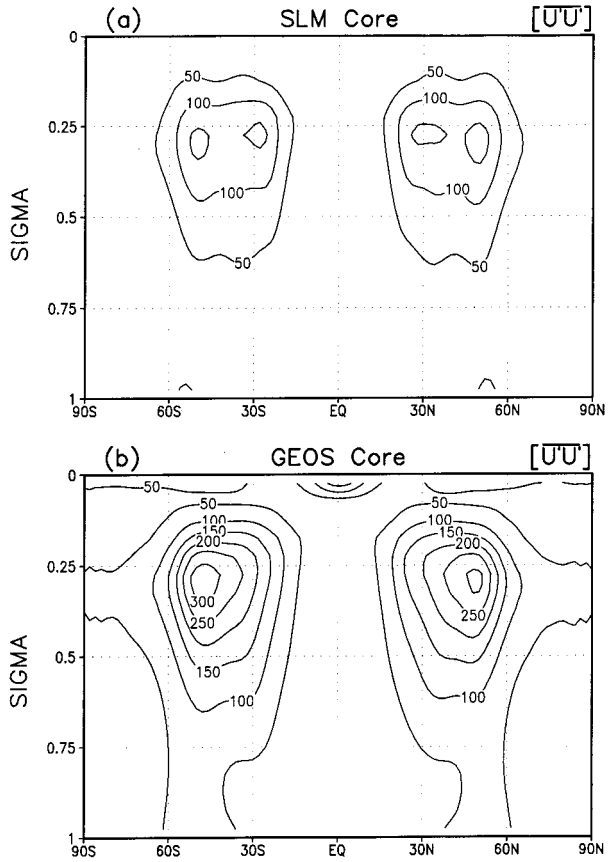


FIG. 12. Time-mean eddy variance of zonal wind from the Held-Suarez tests with the (a) SLM and (b) GEOS dynamical cores. The contour interval is 50 $m^2\ s^{-2}$.

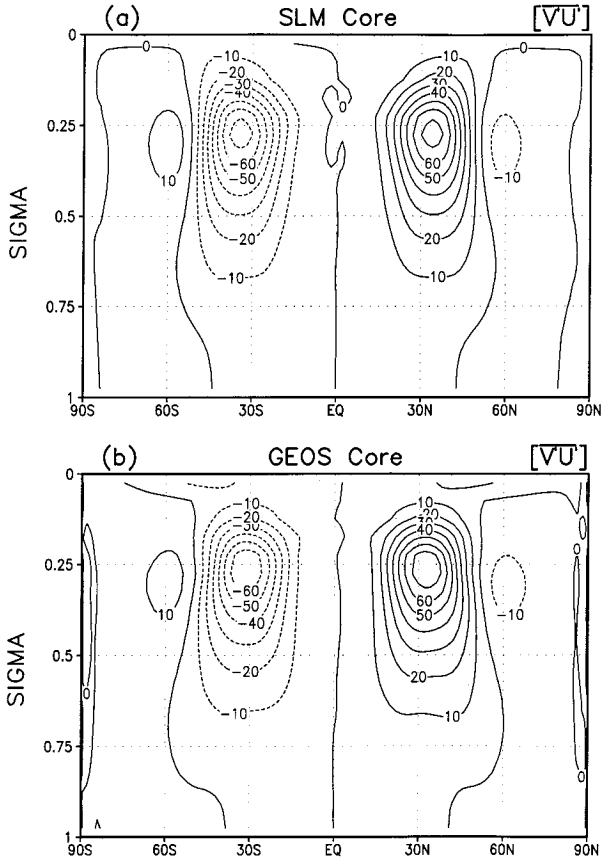


FIG. 13. Time-mean eddy momentum flux from the Held–Suarez tests with the (a) SLM and (b) GEOS dynamical cores. The contour interval is 10 $m^2\ s^{-2}$.

than the GEOS core, but the sign of the difference is opposite. All of these are due to the fact that more waves in the GEOS core propagate to high altitudes before being dissipated and, hence, produce a more vigorous residual circulation, which drives the model away from radiative equilibrium.

The transformed Eulerian mean diagnostics establish that the different attributes of the two dynamical cores do impact the climate characteristics as represented by the Held–Suarez simulations. It is safe to assert that the diffusivity in the SLM core mixes in the lower part of the model, reducing the propagation of wave activity to high altitudes. It remains difficult, however, to link this impact quantitatively back to the climate simulations. The troposphere in the GCM and the atmosphere contains strong local diabatic processes while local heating is not represented in the Held–Suarez test. Because of these local heat sources, diffusivity in the troposphere would have a different impact than in the Held–Suarez test. Given the latitudinal distribution of heat sources, local diffusivity of heat in the GCM would heat the poles.

Direct tests to quantify the role of the diffusion in the two dynamical cores are not simply conceived due to the velocity dependence of the diffusion in the SLM. Possible experiments include adding symmetric diffusion or nonlinear diffusion (Smagorinsky 1963) to the GEOS core. More recent versions of the GEOS GCM include the gravity wave drag scheme of Zhou et al. (1996) (Takacs and Suarez 1996). Gravity wave drag, which is often incorporated into general circulation and numerical weather prediction models to account for zonal wind biases (Palmer et al. 1986; McFarlane 1987), provides a physically motivated momentum mixing process. An experiment using the GEOS GCM with gravity wave drag will be used here to provide heuristic arguments about the role of subgrid processes in the GEOS GCM.

Figure 18 shows the transient eddy heat flux from a simulation of the GEOS GCM with gravity wave drag added. Compared with the climate simulation presented in Fig. 7e, the upper-troposphere maxima in the NH and the SH have been reduced. This makes the GEOS simulation much more similar to the GEOS assimilation (Fig. 7f). Looking at the results from the Held–Suarez test in Fig. 14 suggests that the in situ mixing added by

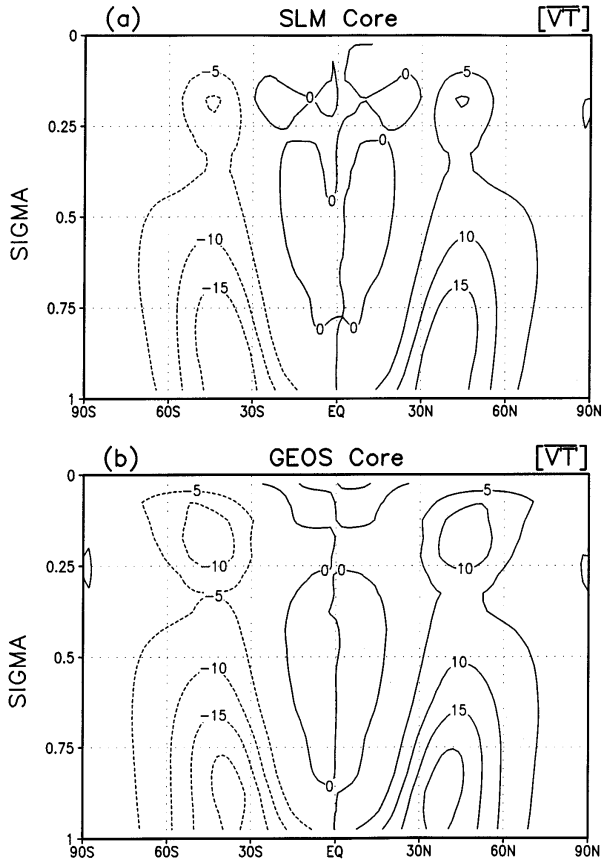


FIG. 14. Time-mean eddy heat flux from the Held-Suarez tests with the (a) SLM and (b) GEOS dynamical cores. The contour interval is 5 K m $s^{-1}$.

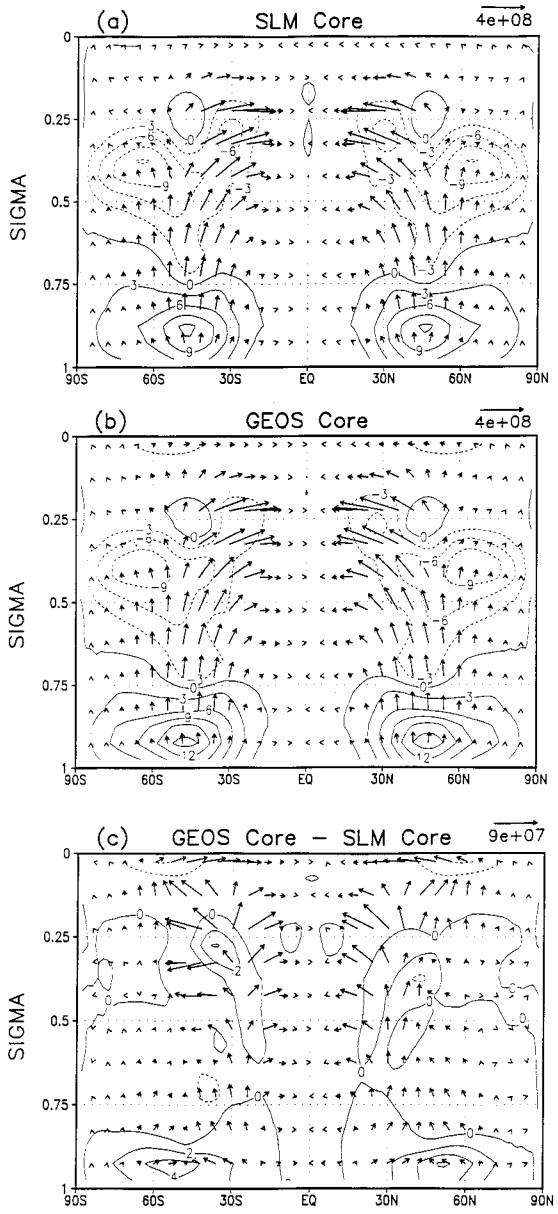


FIG. 15. Vector EP flux and its divergence from the Held-Suarez tests with the (a) SLM and (b) GEOS dynamical cores, and (c) their differences (GEOS − SLM). The contour interval is 3 m $s^{-1}$ $day^{-1}$ in (a) and (b) and 2 m $s^{-1}$ $day^{-1}$ in (c). The flux is in the unit of kg $s^{-2}$. The vertical component of the flux is multiplied by a factor of 100 to make proper vector plots.

the gravity wave drag parameterization and the numerical mixing in the SLM core have a qualitatively similar impact on the eddy heat flux. Therefore, the behavior of the SLM simulation can be safely asserted to be linked to numerical diffusion.

Earlier it was mentioned that the temperature distributions in the Held–Suarez tests (Fig. 11) are in paradox with those in the climate simulations reported in Chen and Bates (1996a). Namely, in the Held–Suarez tests the polar temperature in the upper troposphere from the SLM core is colder than the GEOS core while in the climate simulations the temperature is warmer. Chen and Bates (1996a) have found that the warmer polar temperature in the SLM is due to the more efficient poleward heat transport in the SLM. Both large-scale circulation (mean flow and eddies) and subgrid mixing contribute to the heat transport. Chen and Bates (1996a) have shown that the SLM has a stronger heat transport by the large-scale circulation. On the other hand, the subgrid mixing in the SLM also diffuses heat poleward and results in a stronger poleward heat transport. The relative contributions by the large-scale circulation and the subgrid mixing are unclear yet. The in situ diffusion, however, reduces the Rossby wave action that propagates upward as revealed in the Held–Suarez test. The higher polar temperature in the Held–Suarez test from the GEOS core arises because the more vigorous Rossby wave activity is dissipated in the upper levels of the model, hence inducing stronger downward motion over the poles. The paradox is resolved by climate simulations with a 70-layer version of the GEOS GCM with mesospheric gravity wave drag, which simulates warm-

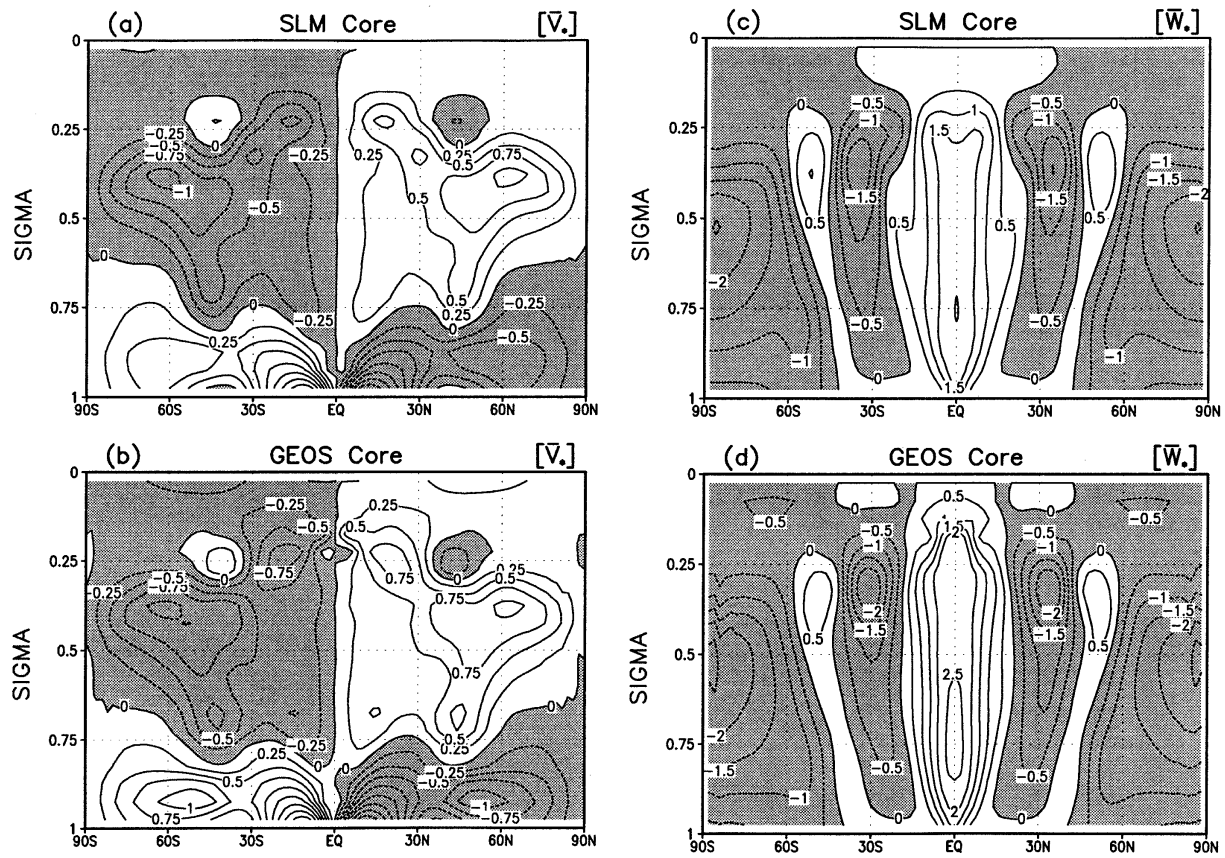


FIG. 16. Residual circulation from the Held-Suarez tests: meridional velocity in the (a) SLM and (b) GEOS dynamical cores and vertical velocity in the (c) SLM and (d) GEOS cores. The contour interval is 0.25 m $s^{-1}$ in (a) and (b) and $0.5 \times 10^{-3}$ m $s^{-1}$ in (c) and (d), with negative values shaded.

er polar temperatures than either of the climate simulations reported by Chen and Bates (1996a) due to the increased residual circulation. This is consistent with the well-known sensitivity of polar temperature in stratospheric modeling as discussed in, for example, Boville (1991, 1995).

## 6. Conclusions

The eddy statistics from the 5-yr climate simulations with the semi-Lagrangian and Eulerian models are evaluated with the 5-yr assimilation from the GEOS data assimilation system. Significant differences between the two simulations are evident, and neither can be declared more accurate in all aspects based on the comparison with the assimilation. Generally, the stationary eddy variances are stronger in the SLM while the transient eddy variances are stronger in the GEOS GCM. The GEOS GCM simulation has no obvious advantage over the SLM simulation, even though the GEOS GCM is used in the GEOS data assimilation system and the physical parameterizations used for the two models have been developed in concert with the GEOS dynamical core. In fact, the SLM simulation is closer to the assimilation than the GEOS GCM simulation in many statistics. This clearly demonstrates that using an assimilation with the same model does not corrupt evaluation of the model, rather it leads to a more controlled environment for studying model shortcomings.

The idealized Held–Suarez test was used to investigate the performance of the two dynamical cores. The eddy statistics are weaker and more diffused in the SLM core than in the GEOS core. This may be due to the much longer time step (1 h vs 3.75 min), the uncentering parameter, and inherent diffusion due to the interpolation in the SLM. The transformed Eulerian mean diagnostics reveal that less wave activity propagates from the lower and middle into the upper parts of the model atmosphere in the SLM core than in the GEOS core. Also in the SLM core, less wave activity propagates equatorward in the upper troposphere. Thus the residual circulation driven by the eddy forcing is weaker in the SLM core than in the GEOS core. Consequently, the SLM is closer to the radiative equilibrium state than the GEOS in the Held–Suarez test. Thus the manner in which the two cores treat small-scale processes impacts

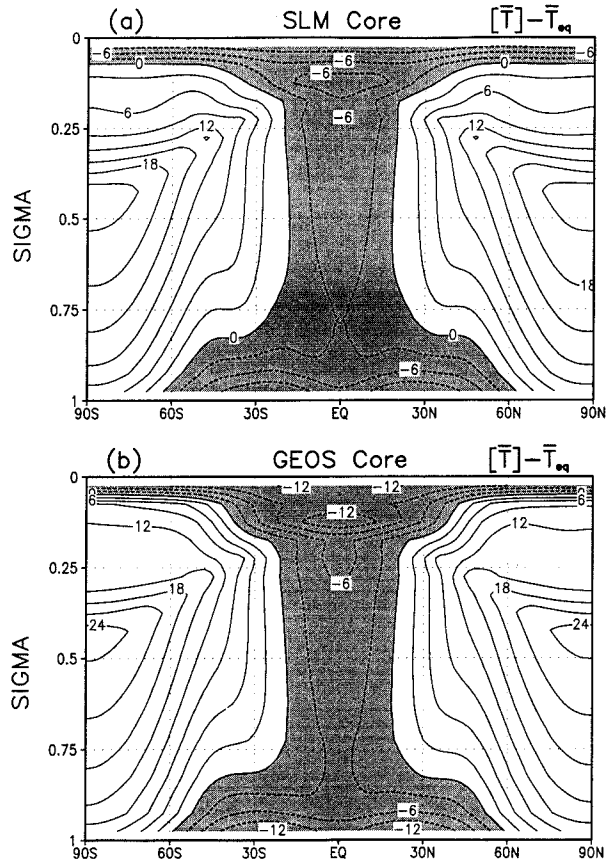


FIG. 17. Difference between the time-mean temperature and the corresponding equilibrium temperature in the Held-Suarez tests with the (a) SLM and (b) GEOS dynamical cores. The contour interval is 3 K with negative values shaded.

the simulation of mean general circulation of the models.

The results from the Held–Suarez simulations, however, cannot be easily applied to the real climate simulations since the mechanisms to maintain the circulation are different in the Held–Suarez test and the atmosphere. The processes for the maintenance of the Held–Suarez circulation are due to action-at-a-distance mechanisms, while local heating in the troposphere is more important in both the GCMs and the atmosphere. The second-order diagnostics from the Held–Suarez test, combined with the gravity wave drag experiment with the GEOS GCM, provide heuristic evidence that the matter in which the two dynamical cores treat small-scale processes, especially diffusion, has a significant impact on the climate simulations. The experiments, therefore, highlight the need for careful physically based parameterizations to model subgrid mixing due to advective cascade. In addition, the subgrid mixing, which is often modeled by filters or diffusion, must also be rationalized with parameterizations that represent subgrid processes such as gravity wave drag.

In this paper we have tried to trace the difference between the two climate simulations to particular characteristics of the dynamical cores. This is motivated by the need to better quantify sources of uncertainties in climate models. In particular, the definition of uncertainties must progress beyond ad hoc attributions to differences in model parameterizations, and the implicit surrender that the uncertainties cannot be better characterized. This study shows the difficulty in chasing down the quantification of performance differences of different models even in a relatively controlled environment of like models, assimilated datasets, and interchangeable parameterization packages. Continual progress will require increased rigor in the definition of controlled experiments.

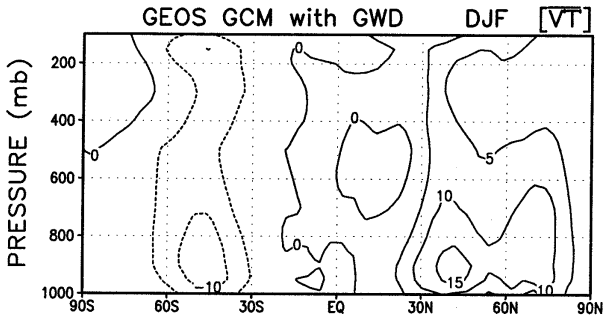


FIG. 18. The DJF transient eddy heat flux from the GEOS GCM simulation with gravity wave drag. The contour interval is 5 K m $s^{-1}$.

*Acknowledgments.* We are grateful to P. Newman and G. Lou for useful discussions on residual circulation dynamics. RBR acknowledges clarifying conversations with T. Sheppard, R. Laprise, N. McFarlane, and J. Mahlman following oral presentations of some of the material in the paper. We also thank anonymous reviewers for valuable comments. This research was supported by the NASA EOS Interdisciplinary Project ''Development and Use of a Four-Dimensional Atmosphere-Ocean-Land Data Assimilation for EOS'' and the NASA Global Modeling and Analysis Program.

## REFERENCES

Andrews, D. G., and M. E. McIntyre, 1976: Planetary waves in horizontal and vertical shear: The generalized Eliassen–Palm relation and the mean zonal acceleration. *J. Atmos. Sci.*, **33,** 2031–2048.

——, J. R. Holton, and C. B. Leovy, 1987: *Middle Atmospheric Dynamics.* International Geophysical Series, Vol. 40, Academic Press, 489 pp.

Arakawa, A., and M. J. Suarez, 1983: Vertical differencing of the primitive equations in sigma coordinates. *Mon. Wea. Rev.*, **111,** 34–45.

Bates, J. R., F. H. M. Semazzi, R. W. Higgins, and S. R. M. Barros, 1990: Integration of the shallow water equations on the sphere using a vector semi-Lagrangian scheme with a multigrid solver. *Mon. Wea. Rev.*, **118,** 1615–1627.

——, S. Moorthi, and R. W. Higgins, 1993: A global multilevel atmospheric model using a vector semi-Lagrangian finite-dif-

ference scheme. Part I: Adiabatic formulation. *Mon. Wea. Rev.*, **121,** 244–263.
Bermejo, R., 1990: On the equivalence of semi-Lagrangian advective schemes and particle-in-cell finite element methods. *Mon. Wea. Rev.*, **118,** 979–987.
Boer, G. J., and B. Denis, 1997: Numerical convergence of the dynamics of a GCM. *Climate Dyn.*, in press.
Boville, B. A., 1991: Sensitivity of simulated climate to model resolution. *J. Climate*, **4,** 469–485.
——, 1995: Middle atmospheric version of CCM2 (MACCM2): Annual cycle and interannual variability. *J. Geophys. Res.*, **100,** 9017–9039.
Chen, M., and J. R. Bates, 1996a: A comparison of climate simulations from a semi-Lagrangian and an Eulerian GCM. *J. Climate*, **9,** 1126–1149.
——, and ——, 1996b: Forecast experiments with a global finite difference semi-Lagrangian model. *Mon. Wea. Rev.*, **124,** 1992–2007.
Edmon, H. J., B. J. Hoskins, and M. E. McIntyre, 1980: Eliassen–Palm cross sections for the troposphere. *J. Atmos. Sci.*, **37,** 2600–2616.
Fels, S. B., J. D. Mahlman, M. D. Schwarzkopf, and R. W. Sinclair, 1980: Stratospheric sensitivity to perturbations in ozone and carbon dioxide: Radiative and dynamical response. *J. Atmos. Sci.*, **37,** 2265–2297.
Harshvardhan, R. Davies, D. A. Randall, and T. G. Corsetti, 1987: A fast radiation parameterization for atmospheric circulation models. *J. Geophys. Res.*, **92,** 1009–1016.
Haynes, P. H., C. J. Marks, M. E. McIntyre, T. G. Shepherd, and K. P. Shine, 1991: On the ''downward control'' of extratropical circulations by eddy-induced mean zonal forces. *J. Atmos. Sci.*, **48,** 651–678.
Held, I. M., and M. J. Suarez, 1994: A proposal for the intercomparison of the dynamical cores of atmospheric circulation models. *Bull. Amer. Meteor. Soc.*, **75,** 1825–1830.
Helfand, H. M., and J. C. Labraga, 1988: Design of a non-singular level 2.5 second-order closure model for the prediction of atmospheric turbulence. *J. Atmos. Sci.*, **45,** 113–132.
Holton, J. R., 1992: *An Introduction to Dynamic Meteorology*. International Geophysical Series, Vol. 48, 3 ed., Academic Press, 511 pp.
——, P. H. Haynes, M. E. McIntyre, A. R. Douglas, R. B. Rood, and L. Pfister, 1995: Stratosphere–troposphere exchange. *Rev. Geophys.*, **33,** 403–439.
Kuo, H.-C., and R. T. Williams, 1990: Semi-Lagrangian solutions to the inviscid Burgers equation. *Mon. Wea. Rev.*, **118,** 1278–1288.
McCalpin, J. D., 1988: A quantitative analysis of the dissipation inherent in semi-Lagrangian advection. *Mon. Wea. Rev.*, **116,** 2330–2336.
McFarlane, N. A., 1987: The effect of orographically excited gravity wave drag on the general circulation of the lower stratosphere and troposphere. *J. Atmos. Sci.*, **44,** 1775–1800.
Moorthi, S., and M. J. Suarez, 1992: Relaxed Arakawa–Schubert: A parameterization of moist convection for general circulation models. *Mon. Wea. Rev.*, **120,** 978–1002.
——, R. W. Higgins, and J. R. Bates, 1995: A global multilevel atmospheric model using a vector semi-Lagrangian finite-difference scheme. Part II: Version with physics. *Mon. Wea. Rev.*, **123,** 1523–1541.
Ostiguy, L., and J. P. R. Laprise, 1990: On the positivity of mass in commonly used numerical flux schemes. *Atmos.–Ocean*, **28,** 147–161.
Palmer, T. N., G. J. Shutts, and R. Swinbank, 1986: Alleviation of a systematic westerly bias in general circulation and numerical weather prediction models through an orographic gravity wave drag parameterization. *Quart. J. Roy. Meteor. Soc.*, **112,** 1001–1039.
Plumb, R. A., and J. D. Mahlman, 1987: The zonally averaged transport characteristics of the GFDL general circulation/transport model. *J. Atmos. Sci.*, **44,** 298–327.
Ritchie, H., C. Temperton, A. Simmons, M. Hortal, T. Davies, D. Dent, and M. Hamrud, 1995: Implementation of the semi-Lagrangian method in a high-resolution version of the ECMWF forecast model. *Mon. Wea. Rev.*, **123,** 489–514.
Schubert, S. D., R. B. Rood, and J. Pfaendtner, 1993: An assimilated dataset for earth science applications. *Bull. Amer. Meteor. Soc.*, **74,** 2331–2342.
——, C.-K. Park, C.-Y. Wu, W. Higgins, Y. Kondratyeva, A. Molod, L. Takacs, M. Seabloom, and R. Rood, 1995: A multiyear assimilation with the GEOS-1 system: Overview and results. NASA Tech. Memo. 104606, Vol. 6, 183 pp.
Smagorinsky, J., 1963: General circulation experiments with the primitive equations: I. The basic experiment. *Mon. Wea. Rev.*, **91,** 99–164.
Staniforth, A., and J. Côté, 1991: Semi-Lagrangian integration schemes for atmospheric models—A review. *Mon. Wea. Rev.*, **119,** 2206–2223.
Suarez, M. J., and L. L. Takacs, 1995: Documentation of the ARIES/GEOS dynamical core, Version 2. NASA Tech. Memo. 104606, Vol. 5, 45 pp.
Sud, Y. C., and A. Molod, 1988: The roles of dry convection, cloud-radiation feedback processes and the influence of recent improvements in the parameterization of convection in the GLA GCM. *Mon. Wea. Rev.*, **116,** 2366–2387.
Takacs, L. L., and M. J. Suarez, 1996: Dynamical aspects of climate simulations using the GEOS general circulation model. NASA Tech. Memo. 104606, Vol. 10, 56 pp.
——, A. Molod, and T. Wang, 1994: Documentation of the Goddard Earth Observing System (GEOS) general circulation model—Version 1. NASA Tech. Memo. 104606, Vol. 1, 100 pp.
Williamson, D. L., and J. G. Olson, 1994: Climate simulations with a semi-Lagrangian version of the NCAR Community Climate Model. *Mon. Wea. Rev.*, **122,** 1594–1610.
World Meteorological Organization, l986: Atmospheric ozone 1985. WMO Global Ozone Research and Monitoring Project Rep. 16, 392 pp.
Zhou, J., Y. C. Sud, and K.-M. Lau, 1996: Impact of orographically induced gravity wave drag in the GLA GCM. *Quart. J. Roy. Meteor. Soc.*, **122,** 903–927.